Revision 1

Effect of correlation between traction forces on tensional homeostasis in clusters of endothelial cells and fibroblasts

Juanyong Li[a,†], Paul E. Barbone[a], Michael L. Smith[b], Dimitrije Stamenović[b,c,*]

[a]Department of Mechanical Engineering, Boston University, Boston, MA 02215

[b]Department of Biomedical Engineering, Boston University, Boston, MA 02215

[c]Division of Material Science and Engineering, Boston University, Brookline, MA 02446

Running head: Correlation of traction forces and tensional homeostasis in cell clusters

Key words: tensional homeostasis, traction forces, focal adhesions, coefficient of variation, correlation

***Corresponding Author**
Dimitrije Stamenović
Department of Biomedical Engineering
Boston University
44 Cummington Mall
Boston, MA 02215
Phone: (617) 353-5902
Fax: (617) 353-6766
E-mail: dimitrij@bu.edu

†Current address:
Juanyong Li
Department of Biomedical Engineering
Worcester Polytechnic Institute
60 Prescott Street
Worcester, MA 01605

Abstract

The ability of cells to maintain a constant level of cytoskeletal tension in response to external and internal disturbances is referred to as tensional homeostasis. It is essential for the normal physiological function of cells and tissues, and for protection against disease progression, including atherosclerosis and cancer. In previous studies, we defined tensional homeostasis as the ability of cells to maintain a consistent level of cytoskeletal tension with low temporal fluctuations. In those studies, we measured temporal fluctuations of cell-substrate traction forces in clusters of endothelial cells and of fibroblasts. We observed those temporal fluctuations to decrease with increasing cluster size in endothelial cells, but not in fibroblasts. We quantified temporal fluctuation, and thus homeostasis, through the coefficient of variation (*CV*) of the traction field; the lower the value of *CV*, the closer the cell is to the state of tensional homeostasis. This metric depends on correlation between individual traction forces. In this study, we analyzed the contribution of correlation between traction forces on traction field *CV* in clusters of endothelial cells and fibroblasts using experimental data that we had obtained previously. Results of our analysis showed that positive correlation between traction forces was detrimental to homeostasis, and that it was cell type-dependent.

1. Introduction

Adherent cells exhibit the remarkable ability to adapt to applied mechanical stresses and strains. Because of this adaptation, cells can maintain their endogenous cytoskeletal mechanical tension at a steady and stable (homeostatic) level, which is essential for the normal physiological function of the tissues (Bazoni and Dejana 2004; Butcher et al., 2009; Chien, 2007; Gulliot and Lecuit, 20013; Humphrey, 2008a, 2008b; Macara et al, 2014; Paszek et al., 2005) and for protection against diseases (Chien, 2007; Paszek et al., 2005; Provenzano and Keely, 2011).

The idea of tensional homeostasis of cells was introduced more than two decades ago (Brown et al., 1998). However, there have been very few quantitative studies of this phenomenon. Mizutani et al. (2004) demonstrated that cellular stiffness returned to a set point level after stretching or relaxing single fibroblasts, which is an indirect indicator of tensional homeostasis in these cells. Webster et al. (2014) have shown that in response to an applied step stretch, isolated fibroblasts do not return to the state of tension that they had prior to the stretch application. The authors referred to their observation as "tensional buffering", rather than tensional homeostasis.

We have studied the dynamic aspect of tensional homeostasis by observing temporal fluctuations of cytoskeletal tension. We defined it as the ability of cells to maintain a consistent level of tension with low temporal fluctuations. By measuring temporal fluctuations of cell-substrate traction forces, we have observed that in some cell types, like in endothelial cells, the traction field exhibits large, erratic temporal fluctuations, which become attenuated in cell clusters, more so, the bigger the number of cells in the cluster (cluster size) is (Canović et al., 2016). On the other hand, in other cell types, like in fibroblasts, cell clustering does not affect traction field variability (Zollinger et al., 2018). In those studies, we used the coefficient of

variation (*CV*) as a quantitative metric of traction field variability. By our definition, the lower the value of *CV* is, the closer the cell to the state of tensional homeostasis is. Although *CV* does not specify a threshold below which tensional homeostasis is achieved, it does permit quantitative comparison to determine how different factors, such as multicellularity, contribute to tensional homeostasis.

By its definition, *CV* depends on the covariance, and therefore on correlation between traction forces. The impact of this correlation on tensional homeostasis of cells has not yet been investigated. In this study, we carried out correlation analysis of our previous experimental data for traction dynamics for clusters of endothelial cells and for clusters of fibroblasts. Results of our analysis might explain why cell clustering promotes tensional homeostasis in endothelial cells and not in fibroblasts.

2. Methods

We consider a cluster of cells which assemble and disassemble focal adhesions (FAs) continuously over time. The traction forces exerted on those FAs are measured at equal time intervals (t_i), where $i = 1,2,\ldots N_t$, and N_t is the total number of time intervals during an observation period. Let $\{\mathbf{x}_k \,|k = 1, 2, \ldots..N_F\}$ be the set of all locations where FAs are formed at *any* time during the observation period and N_F is the number of all FAs. Let $\mathbf{F}(\mathbf{x}_k,t_i)$ be a traction force vector acting on an FA at location $\mathbf{x}_k$ at time t_i. If at t_i there is no recorded force at $\mathbf{x}_k$, then we consider that $\mathbf{F}(\mathbf{x}_k,t_i) = \mathbf{0}$.

We used a scalar metric of the magnitude of the traction field, $T(t_i)$, defined as the sum of magnitudes of all traction force vectors in the cluster at a given t_i, (Canović et al., 2016), i.e.,

$$T(t_i) = \sum_{k=1}^{N_F} \| \mathbf{F}(\mathbf{x}_k, t_i) \|, \tag{1}$$

For simplicity, we will label the magnitude of the traction force at $(\mathbf{x}_k,t_i)$ as $F_k(t_i) \equiv ||\mathbf{F}(\mathbf{x}_k,t)||$.

The coefficient of variation of $T(t_i)$ is defined as follows

$$CV = \frac{\sigma(T)}{\langle T \rangle}, \tag{2}$$

where $\langle T \rangle$ is the time average of $T(t_i)$, i.e.,

$$\langle T \rangle = \frac{1}{N_t}\sum_{i=1}^{N_t} T(t_i), \tag{3}$$

and $\sigma(T)$ is the corresponding standard deviation. The variance is therefore

$$\sigma^2(T) = \frac{1}{N_t}\sum_{i=1}^{N_t}[T(t_i) - \langle T \rangle]^2 = \langle T - \langle T \rangle \rangle^2 = \langle T^2 \rangle - \langle T \rangle^2, \tag{4}$$

By combining Eqs. (1) and (4), we obtain that

$$\langle T^2 \rangle - \langle T \rangle^2 = \frac{1}{N_t}\sum_{i=1}^{N_t}\left(\sum_{k=1}^{N_F} F_k(t_i)\right)\left(\sum_{j=1}^{N_F} F_j(t_i)\right) - \langle T \rangle^2 = \sum_{k=1}^{N_F}\sum_{j=1}^{N_F} \mathrm{cov}(F_k, F_j), \tag{5}$$

where

$$\mathrm{cov}(F_k, F_j) = \frac{1}{N_t}\sum_{i=1}^{N_t}[F_k(t_i) - \langle F_k \rangle][F_j(t_i) - \langle F_j \rangle] \tag{6}$$

is the covariance between forces applied at FAs locations $\mathbf{x}_k$ and $\mathbf{x}_j$ and $\langle \cdot \rangle$ denotes the time average. Thus, it follows from Eqs. (4)-(6) that

$$\sigma^2(T) = \sum_{k=1}^{N_F}\sigma^2(F_k) + \sum_{k \neq j=1}^{N_F \times (N_F - 1)} \mathrm{cov}(F_k, F_j), \tag{7}$$

where $\sigma^2(F_k)$ is the variance of the traction force applied at $\mathbf{x}_k$.

By substituting Eqs. (4) and (7) into Eq. (2), we obtain an expression for CV as follows

$$CV = \frac{\sqrt{\sum_{k=1}^{N_F} \sigma^2(F_k) + \sum_{j \neq k=1}^{N_F \times (N_F - 1)} \mathrm{cov}(F_k, F_j)}}{\sum_{k=1}^{N_F} \langle F_k \rangle}. \quad (8)$$

According to Eq. (8), CV of the traction field depends on the variability of traction forces, their correlation and their magnitude.

2.1. Correlation Analysis

For each pair of forces (F_j, F_k) in a cluster, the corresponding correlation coefficient, $r(F_j,F_k)$, is given as follows

$$r(F_j, F_k) = \frac{\sum_{i=1}^{N_t} [F_j(t_i) - \langle F_j \rangle][F_k(t_i) - \langle F_k \rangle]}{N_t \sigma(F_j)\sigma(F_k)} = \frac{\mathrm{cov}(F_j, F_k)}{\sigma(F_j)\sigma(F_k)}. \quad (9)$$

Next, we create a symmetric correlation matrix whose elements are $r(F_j,F_k) = r(F_k,F_j)$, with $j,k = 1,2,\ldots N_F$. According to Eq. (9), the diagonal elements of the matrix all have the value of unity. We then sum all the elements in the matrix and subtract the trace of the matrix (which equals N_F) from that sum. This yields a coefficient of global correlation of all forces in the cluster (R) as follows

$$R = \sum_{j,k=1}^{N_F} r(F_j, F_k) - N_F. \quad (10)$$

Since the number of FAs vary between clusters of the same number of cells, we normalize R by two times the number of combinations ($C_2^{N_F}$) of unrepeated pair of forces among

127 N_F forces, i.e., $C_2^{N_F} = N_F!/2!(N_F-2)!$. The factor of two is because of symmetry of the
128 correlation matrix. Thus, we obtain the normalized global correlation coefficient (R_{norm}) as

129 $$R_{norm} = \frac{R}{2C_2^{N_F}} = \frac{R}{N_F(N_F-1)}. \quad (11)$$

130 Note that R_{norm} is the average Pearson's correlation coefficient of each pair of forces. If $0 < R_{norm}$
131 ≤ 1, all forces in a cluster are predominantly positively correlated, if $-1 \leq R_{norm} < 0$, all forces in
132 a cluster are predominantly negatively correlated, and if $R_{norm} = 0$, forces are not correlated.

133 2.2. Data Analysis

134 We used experimental data that we obtained from traction microscopy on single cells and
135 on multicellular clusters of bovine aortic endothelial cells (BAECs) and of mouse embryonic
136 fibroblasts (MEFs) (Canović et al., 2016; Zollinger et al., 2018). A brief description of the
137 traction microscopy technique is given below.

138 Cellular traction forces are measured by plating cells on soft polyacrylamide gels whose
139 apical surface is micropatterned by a regular array of fibronectin dots (2-μm diameter and 6 μm
140 center-to-center spacing). Those dots are loci where cells form FAs. By observing motion of
141 dots in response to cell contraction and from known elastic properties of the gel, we can compute
142 traction forces applied to individual FAs (Polio et al., 2012, 2014).

143 Traction forces were measured at 5 min intervals over 2 h, i.e., $N_t = 25$. The cluster size
144 ranged from 2 to 30 cells in BAECs and 3 to 17 cells in MEFs. Altogether, there were 63 single
145 cells and clusters in BAECs and 30 single cells and clusters in MEFs. Since the clusters were
146 freely formed, the number of FAs varied between single cells and between clusters having the
147 same number of cells.

In the present analysis, we tracked each fibronectin dot within a cluster where an FA was formed during the observation time. If the force applied at the FA fell below the experimental threshold of 0.3 nN (Polio et al., 2012), we assigned it a zero value. The total number of traction forces within the cluster was equal to the average number, N_F, of active FAs observed during 2 h.

In order to quantify the effect of correlation between traction forces on the traction field variability, we compared values of *CV* obtained from clusters with measured traction forces, with values of *CV* obtained from clusters with simulated uncorrelated traction forces. The latter were obtained as follows.

We randomized fluctuations of measured traction forces as follows. Each time lapse of a traction force measured over 2 h at a 5-min sampling rate represents a sequence of 25 forces: $F(t_1)$, $F(t_2)$, $F(t_3)$,…. $F(t_{25})$. Using a MATLAB random number generator, we reordered integers 1 to 25 and then, accordingly created a random sequence of 25 forces from a measured sequence of forces. This procedure did not alter values of $\sigma(F)$ and $\langle F \rangle$, while at the same time it reduced temporal correlation between traction forces that may have existed before reordering. In each cluster, measured forces were replaced by the corresponding simulated uncorrelated forces, and *CV* was computed as above.

3. Results

We found that the contribution of correlation between traction forces was different in clusters of BAECs than in clusters of MEFs. In both BAECs and MEFs, application of simulated uncorrelated forces caused *CV* to decrease relative to the values obtained with measured forces. This decrease was greater in BAECs, roughly 50% on average over the entire range of N_F (Fig. 1a), than in MEFs, where it was < 50% (Fig. 1b).

In the clusters of BAECs with measured forces, CV exhibited a significant negative dependence on N_F (Spearman correlation coefficient $\rho = -0.404$, $p = 0.0011$), which followed a power-law relationship, $CV = 1.06N_F^{-0.47}$ (Fig. 2a). When we applied uncorrelated forces, CV also exhibited a significant negative dependence on N_F ($\rho = -0.671$, $p = 2\times10^{-7}$) and also followed a power law, $CV = 0.62N_F^{-0.5}$ (Fig. 2a). In the clusters of MEFs with measured forces, CV was virtually independent of N_F ($\rho = 0.016$, $p = 0.931$) (Fig. 2b). When uncorrelated forces were applied, however, the CV vs. N_F relationship exhibited a nearly significant negative dependence ($\rho = -0.344$, $p = 0.062$), which followed a power law, $CV = 0.49N_F^{-0.56}$ (Fig. 2b).

In BAECs, R_{norm} decreased with increasing N_F for lower values of N_F, and exhibited no systematic dependence for larger values of N_F (Fig. 3), whereas in MEFs, R_{norm} slightly decreased with increasing N_F from the mid-range of N_F (Fig. 3). This is consistent with the data for measured forces shown in Fig. 1.

The average values shown in Figs. 1 and 3 were calculated by dividing the range of N_F into bins of ten. Bins with fewer than three data points were not taken into consideration.

4. Discussion

In this exercise, we analyzed the impact of correlation between traction forces on tensional homeostasis of multicellular clusters of BAECs and MEFs. We found that correlation between FA forces was detrimental for homeostasis and that it had different effects on these two cell types. In BAECs, the correlation enhanced traction field variability and decreased with increasing N_F, which is consistent with our previous observation that CV decreases with increasing cluster size. In MEFs, however, the correlation had a lesser effect on traction field variability than in BAECs and changed little with increasing N_F, which is consistent with our

192 previous observation that CV does not change with increasing cluster size. These are novel and
193 the most significant findings of this study.

194 The observed correlation between traction forces may be explained by the fact that these
195 forces must be balanced at all times. Any perturbation that disturbs force balance must be
196 accompanied by a simultaneous, correlated force readjustment in order to reestablish
197 equilibrium. This, however, does not explain the observed lower correlation of traction forces in
198 MEFs than in BAECs, which may be associated with more random force fluctuations in MEFs
199 than in BAECs.

200 From a biological point of view, it is reasonable to expect that in BAECs increasing N_F is
201 favorable for achieving tensional homeostasis. These cells form monolayers *in vivo* where a
202 very large N_F may overcome the detrimental effect of correlation between traction forces on
203 tensional homeostasis. In MEFs, however, increasing N_F appears to have a little effect on
204 tensional homeostasis. This, in turn, suggests that MEFs need to be able to achieve tensional
205 homeostasis at a single cell level, which is consistent with the fact that these cells *in vivo* do not
206 form large clusters and monolayers.

207 In conclusion, this study highlights the impact of correlation between FA traction forces
208 on the ability of cells to achieve tensional homeostasis. This impact appears to be cell-type
209 dependent and in accordance with biological functions of cells. This study also provides a
210 quantitative tool to analyze traction force data and to compare the contractile behavior of
211 different cell types and its evolution with the size of the cell clusters.

212

213

Declaration of Competing Interest

The authors declare no conflicts of interest.

Acknowledgements

We thank Dr. Han Xu for providing experimental data. This study was supported by NSF grants CEBET 115467 (M. L. Smith), CMMI-1362922 and CMMI-1910401 (D. Stamenović).

References

Bazoni, G., Dejana, D. 2004. Endothelial cell-to-cell junctions: molecular organization and role in vascular homeostasis. Physiol. Rev. 84, 869-901.

Brown, R. A., Prajapati, R., McGrouther, D. A., Yannas, I. V., Eastwood, M. 1998. Tensional homeostasis in dermal fibroblasts: mechanical responses to mechanical loading in three-dimensional substrates. J. Cell Physiol. 175, 323-332.

Butcher, D. T., Alliston, T., Weaver, V. M., 2009. A tense situation: forcing tumor progression Nat. Rev. Cancer 9, 108-122.

Canović, E. P., Zollinger, A. J., Tam, S. N., Smith, M. L., Stamenović, D. 2016. Tensional homeostasis in endothelial cells is a multicellular phenomenon. Am. J. Physiol. Cell Physiol. 311, C528-C535.

Chien, S. 2007. Mechanotransduction and endothelial cell homeostasis: the wisdom of the cell. Am. J. Physiol. Heart Circ. Physiol. 292, H1209-H1224.

Guillot, C, Lecuit, T. 2013. Mechanics of epithelial tissue homeostasis and morphogenesis. Science 340, 1185-1189.

Humphrey, J. D. 2008a. Mechanism or arterial remodeling in hypertension: coupled roles of wall shear and intramural stress. Hypertension 52, 195-200.

Humphrey, J. D. 2008b. Vascular adaptation and mechanical homeostasis at tissue, cellular, and subcellular levels. Cell Biochem. Biophys. 50, 53-78.

Macara, I. G., Guyer, R., Richardson, G., Huo, Y., Ahmed, M. 2014. Epithelial homeostasis. Curr. Biol. 24, R815-R825.

Mizutani, T., Haga, H., Kawabata, K. 2004. Cellular stiffness response to external deformation: tensional homeostasis in a single fibroblast. Cell Motil. Cytoskeleton 59, 242-248.

Paszek, M. J., N. Zahir, K. R. Johnson, J. N. Lakins, G. I. Rozenberg, A. Gefen, C. A. Reinhart-King, S. S. Margulies, M. Dembo, D. Boettiger, D. A. Hammer, V. M. Weaver. 2005. Tensional homeostasis and the malignant phenotype. Cancer Cell 8, 241-254.

Polio, S. R., Parameswaran, H., Canović, E. P., Gaut, C. M., Aksyonova, D., Stamenović, D., Smith, M. L. 2014. Topological control of multiple cell adhesion molecules for traction force microscopy. Integr. Biol. 6, 357-365.

Polio, S. R., Rotheneberg, K. E., Stamenović, D. Smith, M. L. 2012. A micropatterning and image processing approach to simplify measurement of cellular traction forces. Acta Biomater. 8, 82-88.

Provenzano, P. P., Keely, P. J. 2011. Mechanical signaling through the cytoskeleton regulates cell proliferation by coordinated focal adhesion and Rho GTPase signaling. J. Cell Sci. 124: 1195-1205.

Webster, K. D., Ng, W. P., Fletcher, D. A. 2014. Tensional homeostasis in single fibroblasts. Biophys. J. 107, 146-155.

Zollinger, A. J., Xu, H., Figueiredo, J., Paredes, J., Seruca, R., Stamenović, D., Smith, M. L. 2018. Dependence of tensional homeostasis on cell type and on cell-cell interactions. Cell. Mol. Bioeng. 11, 175-184, 2018.

Figure Captions

Figure 1. Relative contribution of correlation on of FA forces to the coefficient of variation of the traction field (CV) in clusters of BAECs (a) and in clusters of MEFs (b). Light gray indicate the contribution of measured forces and the dark gray indicates the contribution of simulated uncorrelated forces. Data are mean ± SE; * indicates significantly higher values of CV obtained from measured forces relative to values obtained from uncorrelated forces ($p < 0.05$). The data were analyzed using the one-tailed paired t-test, or the Wilcoxon signed-rank test if the data failed the normality (Shapiro-Wilk) test.

Figure 2. Relationships between the coefficient of variation of the traction field (CV) and the total number of focal adhesions (N_F) in clusters of BAECs (a) and MEFs (b) with measured traction forces (open circles) and with uncorrelated traction forces (solid circles) with the solid and the dashed lines representing the best fit of the power-law relationship, respectively.

Figure 3. Relationships between the normalized global correlation coefficient (R_{norm}) and the total number of focal adhesions (N_F) in clusters of BAECs (solid circles) and MEFs (open circles). Data are average ± SE; * indicates lower values of R_{norm}, which are marginally significant ($p < 0.1$), relative to its highest value in BAECs, and # indicates lower values of R_{norm}, which are marginally significant ($p < 0.1$), relative to its highest value in MEFs. The data were analyzed using the one-tailed t-test, or the Mann-Whitney rank-sum test if the data failed the equal variance (Brown-Forsythe) test.

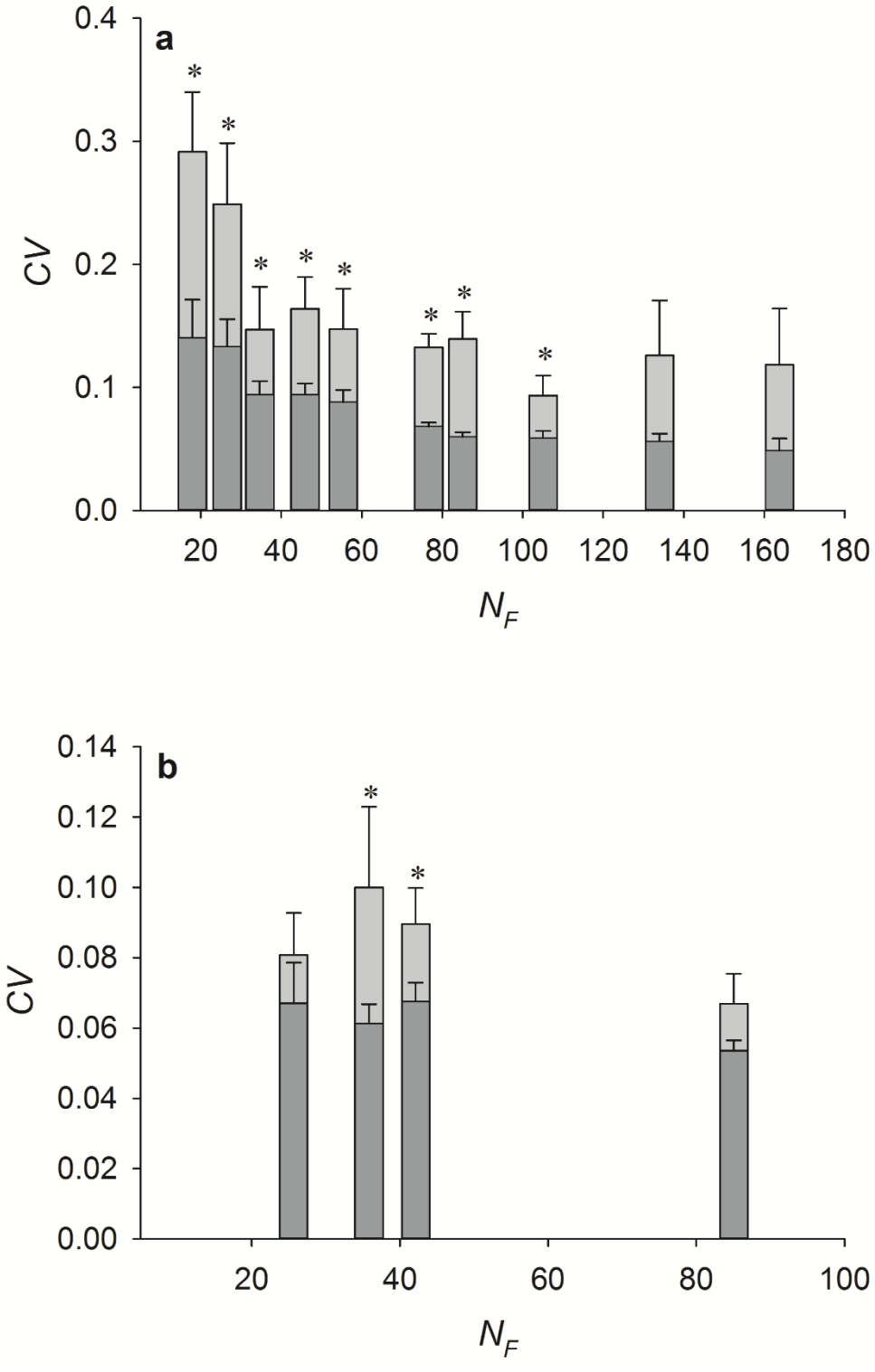
a
0.4
0.3
0.2
0.1
0.0
CV
20
40
60
80
100
120
140
160
180
N_F
b
0.14
0.12
0.10
0.08
0.06
0.04
0.02
0.00
CV
20
40
60
80
100
N_F

Figure 1

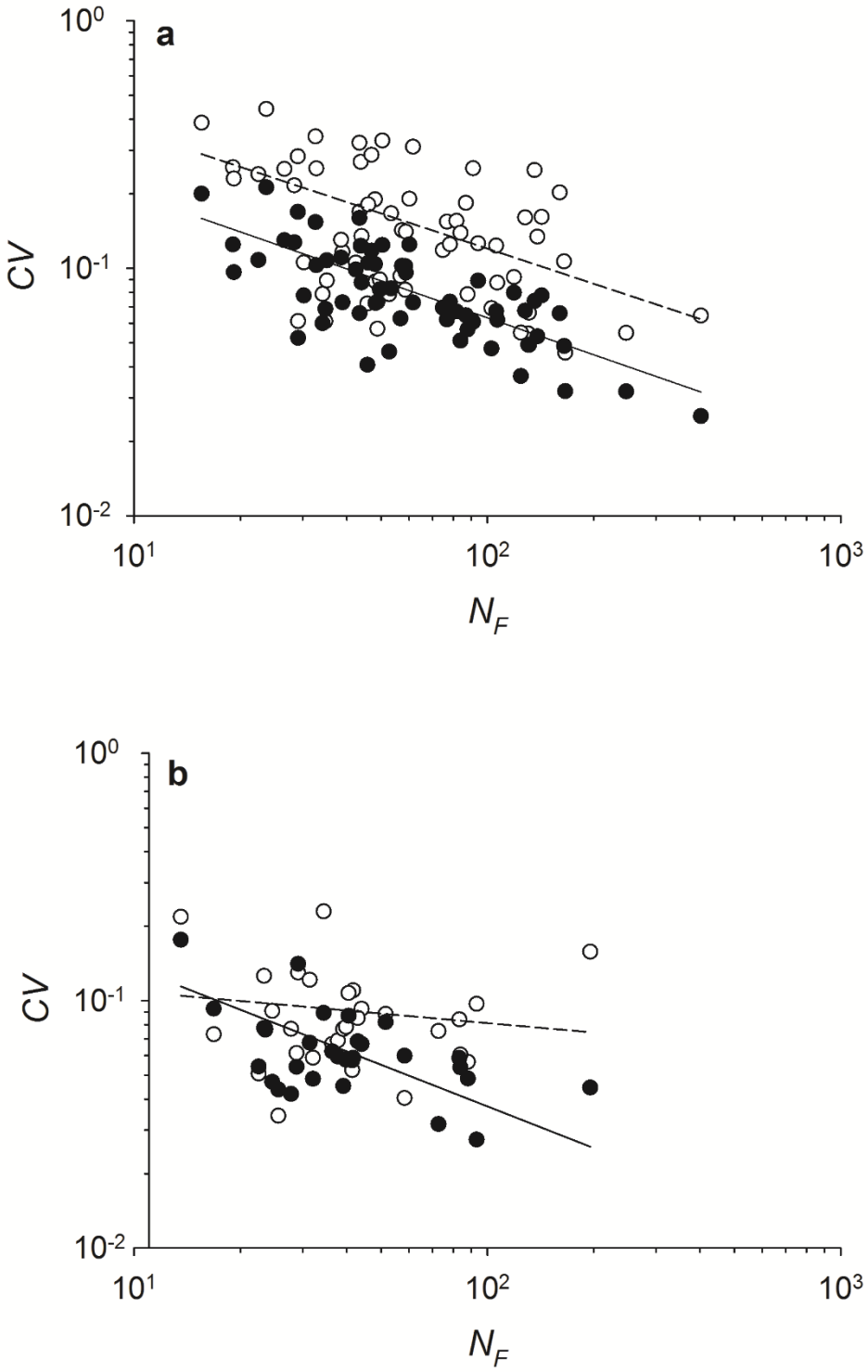

Figure 2

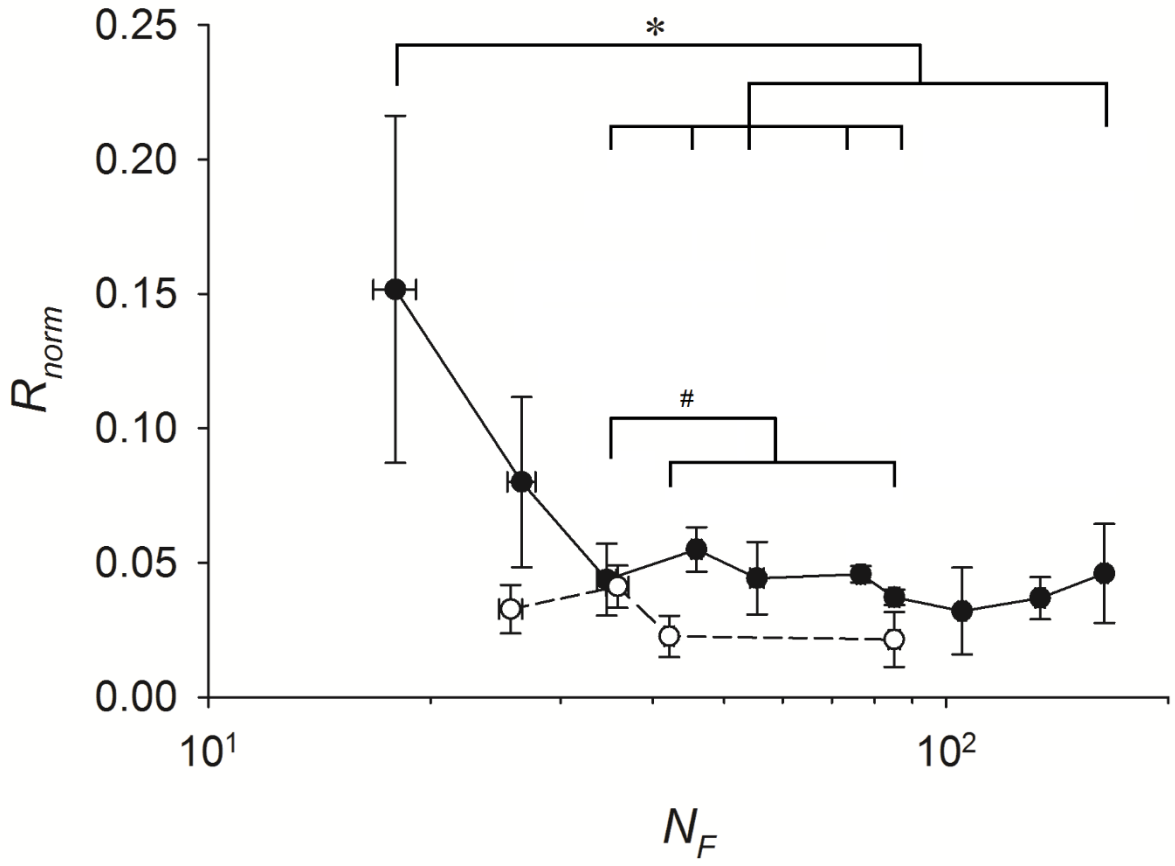

337

338 Figure 3